Charcoal Morphometry for Paleoecological Analysis: The Effects of Fuel Type and Transportation on Morphological Parameters

Authors: Crawford, Alastair J., and Belcher, Claire M.

Source: Applications in Plant Sciences, 2(8)

Published By: Botanical Society of America

URL: https://doi.org/10.3732/apps.1400004

Applications in Plant Sciences 2014 2(8): 1400004

Application Article

Charcoal morphometry for paleoecological analysis: The effects of fuel type and transportation on morphological parameters[1]

Alastair J. Crawford[2] and Claire M. Belcher[2,3]

[2]Earth System Science Group, College of Life and Environmental Sciences, University of Exeter, Level 7 Laver Building, North Park Road, Exeter EX4 4QE, United Kingdom

- *Premise of the study:* Charcoal particles preserved in sediments are used as indicators of paleowildfire. Most research focuses on abundance as an indicator of fire frequency, but charcoals also convey information about the vegetation from which they are derived. One potential source of information is their morphology, which is influenced by the parent material, the nature of the fire, and subsequent transportation and burial.
- *Methods:* We charcoalified 26 materials from a range of plant taxa, and subjected them to simulated fluvial transport by tumbling them with water and gravel. We photographed the resulting particles, and used image analysis software to measure morphological parameters.
- *Results:* Leaf charcoal displayed a logarithmic decrease in area, and a logarithmic increase in circularity, with transportation time. Trends were less clear for stem or wood charcoal. Grass charcoal displayed significantly higher aspect ratios than other charcoal types.
- *Conclusions:* Leaf charcoal displays more easily definable relationships between morphological parameters and degree of breakdown than stem or wood charcoal. The aspect ratios of fossil mesocharcoal can indicate the broad botanical source of an assemblage. Coupled to estimates of charcoal abundance, this will improve understanding of the variation in flammability of ancient ecosystems.

Key words: charcoal morphology; fire history; image analysis; mesocharcoal; taphonomy.

Charcoal is a carbonaceous material formed by pyrolysis when the temperature of any organic material rises above its dry ignition temperature, but is prevented from igniting by hypoxic conditions (Orvis et al., 2005). In a wildfire, heat penetrates ahead of the oxidation reaction, and a layer of charcoal therefore remains at the edge of the burned area when it ceases to spread. Charcoal possesses two characteristics that make it valuable for paleoecological and paleoenvironmental reconstruction: it preserves the anatomy of the source material, and is generally chemically and biologically inert (Scott, 2010). Preservation of anatomy, which may include all parts of the plant, including leaves, flowers, and fruits, as well as woody material (Scott et al., 2000), enables potential taxonomic identification of fossil charcoal samples, and occasionally can allow for inferences to be made about wider environmental parameters, such as climatic information from growth rings (Falcon-Lang, 1999), or atmospheric CO_2 concentration from stomatal density (McElwain, 1998). Charcoal's inert nature allows its preservation in sedimentary environments on geological timescales (Scott and Damblon, 2010), and also makes its extraction from rocks or sediments relatively easy (Mooney and Tinner, 2011). Sedimentary charcoal is therefore widely used in paleoenvironmental studies as an indicator of fire activity (Conedera et al., 2009).

Charcoal used for this purpose may be isolated from terrestrial sediments, peat deposits, soils, or marine sediments. It is normally quantified optically, either as an areal measurement or particle count, and these measures taken as indicative of the prevalence of wildfire at the time the sediment was deposited. Ordinarily a series of samples from different depths will be used, in combination with a dating method, to produce a curve of charcoal influx over time. Peaks in this curve may be interpreted as individual fires, and series of peaks as indicators of fire frequency. However, these interpretations are complicated by uncertainty as to the source area of the charcoal (Peters and Higuera, 2007), the need for temporal resolution of the sampling to exceed fire frequency (Marlon et al., 2009), and potential bias in distinguishing peaks from background variation (Higuera et al., 2010). Changes in charcoal influx may therefore be interpreted as "fire activity"—without making assumptions about the relative contributions of size, frequency, and proximity of fires to the signal (Marlon et al., 2009). It should be noted that charcoal influx may also be affected by variability in the proportion of the burned material that is charcoalified, and potentially by the decay of charcoal post-deposition (Scott and Damblon, 2010), while mixing of sediments post-deposition may also obscure the signal (Whitlock and Millspaugh, 1996).

The distance that charcoal is transported before incorporation into a sedimentary environment is strongly influenced by

[1]Manuscript received 17 January 2014; revision accepted 12 July 2014.

This research was supported by funding from a Marie Curie Career Integration Grant (to C.M.B.; PCIG10-GA-2011-303610).

[3]Author for correspondence: c.belcher@exeter.ac.uk

doi:10.3732/apps.1400004

particle size, whether that transportation occurs by air (Moore, 1989) or by water (Scott, 2010). Smaller particles are more susceptible to aerial transport, and theoretical studies of this (Clark, 1988; Peters and Higuera, 2007; Higuera et al., 2007) have been used to simulate charcoal deposition patterns and elucidate the relative importance of the different factors that affect sedimentary charcoal records. However, Scott (2010) warns that most macroscopic charcoal (>1 mm) undergoes transportation by water, and so cannot be assumed to relate only to local fires.

Understanding these transportation processes is important for the interpretation of charcoal assemblages. While particle size is commonly used to indicate the source area of an assemblage, the possibility that transportation may result in sorting according to morphology (which is likely influenced by botanical affinity) as well as size is not generally addressed. In addition, both particle size and morphology may be altered by the transportation processes themselves. Belcher et al. (2013) have drawn attention to the importance of morphological changes during transport, showing that apparently moderate changes in particle size may strongly affect estimates of the charcoal content of a sediment sample.

An important factor in the utility of charcoal as a paleoecological indicator is its ability to preserve plant anatomy in environments where the material would otherwise decay (Scott, 2010). The broad botanical affinities of mesofossil and microfossil charcoals can be readily identified using a scanning electron microscope (Scott, 2000). Charcoalification leads to three-dimensional preservation of plant cellular structure, which enables characteristic features to be used to identify, for example, wood type. However, it is not practical in terms of time, or in some cases cost, to take scanning electron micrographs of all charcoal particles in an assemblage, and so a number of authors have promoted the idea that the broad morphology of mesocharcoal may be used to indicate the nature of the material from which it was formed. Jensen et al. (2007) identified five morphotypes from a minority of particles that were morphologically distinctive in Holocene lake sediments, and could reproduce four of these to some extent by selection of parent material when producing charcoal under laboratory conditions.

Umbanhowar and McGrath (1998) applied image analysis to particles (125–250 μm and 250–600 μm) of laboratory-created charcoal from eight grass species and the leaves and wood of eight tree species, and discovered significant differences in certain morphological parameters across material types. They suggested that the length : width ratio of charcoal particles might be used to identify their source as either grassland or forest fire. However, there remains a question over whether such a technique is generally applicable, or only when limited to a defined range of potential taxa. In addition, any morphological feature that has value as a paleoecological or paleoenvironmental proxy would likely only remain distinct within a given range of degrees of breakdown, and such techniques would therefore be dependent on understanding the taphonomic history of the charcoal assemblage. A further question arising from such morphometric studies is the extent to which particle morphology is influenced by the method by which larger charcoal pieces have been broken down. Charcoal crushed in a mortar and then sieved, as in Umbanhowar and McGrath (1998), may display different morphological features compared to that broken down by natural processes.

Nichols et al. (2000) simulated the effects of bedload transport by placing charcoal produced from *Pinus sylvestris* L. twigs, sieved to between 3.3 and 9.5 mm, with sand and water in a cylindrical motorized tumbler, before determining the weights of different size fractions. No consistent relationship was found between the period of abrasion and degree of breakdown. Most breakdown occurred rapidly, and appeared to consist in large part of the removal of bark, after which particles remained generally stable. Increasing the proportion of sand increased the abrasion rate only moderately, while the tendency for charcoal to break down did not vary notably between charring temperatures of 450°C, 600°C, and 800°C, but was notably reduced at 250°C. To our knowledge, this has been the only published study on the effects of simulated transport on charcoal particles.

In this study, we aim to determine the effects of charcoal fragmentation on its morphological characteristics; specifically the area, circularity, and aspect ratio of particle images. We have subjected charcoal particles derived from a range of plant materials to a realistic method of breakdown, with the aim of establishing whether different fuel types undergo distinctive changes in morphology under increasing degrees of breakdown. We also further test the hypothesis of Umbanhowar and McGrath (1998) that the aspect ratio of charcoal particles can reveal whether they originate in grassland or woodland fire.

MATERIALS AND METHODS

Specimens of 26 plant materials (Table 1) were obtained from 14 species, consisting of two pteridophytes, eight conifers, two grasses, and two other angiosperms—one weedy and one arborescent. Species were selected with the aim of including a broad range of physical forms and are weighted toward those with a long geological record, because sedimentary charcoal may be found dating back to the Paleozoic era (Glasspool et al., 2004). Conifers were of particular interest to us, because of their long geological history and because they were not included in the experiments of Umbanhowar and McGrath (1998). In most cases, both foliage and stems or branches were sampled. Native species were sampled from locations in southwestern England and northern Wales, and exotic species from the botanical collection at the University of Exeter. Specimens were dried to a constant weight at 50°C before samples were removed. Samples generally consisted of 1-cm lengths of stems, twigs, or long narrow leaves, or 1 × 1-cm squares of broad leaves. The morphology of the specimen determined the exact size and shape of the samples removed. These are given in detail in Appendix S1.

Samples were tightly wrapped in aluminum foil and placed in batches of eight in 75-mL stainless steel crucibles, which were then filled with clean mineral sand of grain size ≤500 μm to exclude oxygen. The crucibles were placed in the center of a Carbolite GLM3 furnace (Carbolite Ltd., Hope Valley, United Kingdom) at 550°C for 20 min, during which time the temperature remained within the range 547–553°C, before being removed from the furnace to cool to room temperature. This produced samples of pure charcoal (Fig. 1A), with no material left uncharred, and with only very slight ash production at the edges of some samples. Noncharcoalified material may have remained at the center of some woody samples.

Each charcoal sample (mass 0.0008–0.1068 g; mean = 0.0191 g; $\sigma = 0.0253$ g) was placed in a 40-mL polypropylene tube (30 × 70 mm) with a polyethylene screw-cap. Approximately 10 g (9.71–10.36 g; mean = 9.96 g; $\sigma = 0.10$ g) of silicate gravel (mass 0.07–1.02 g; mean = 0.33 g; $s = 0.17$ g) was added, and the tube filled with tap water (Fig. 1B). Sample tubes were affixed to an electric motor, at 10 cm from the axis of rotation and aligned tangential to the direction of rotation, and turned over at 47 revolutions per minute for periods of between one and eight hours. The speed of rotation is arbitrary, but low enough to avoid any inertial displacement of the contents of the tube. Samples were sieved at 125 μm, and the gravel removed. The charcoal particles retained on the sieve were dispersed in water in 55-mm Petri dishes and left at room temperature for the water to evaporate (Fig. 1C).

The particles were then imaged using a dissecting microscope and Tucsen ISH500 digital camera with View version 7.1.1.7 imaging software (Xintu Photonics Co. Ltd., Fuzhou, Fujian, China). Where the original woody particle remained largely intact, this was removed prior to imaging. An area of 16 cm^2

Table 1. Species and material types used for the production of charcoal.

Species	Leaf	Wood	Non-woody stem	Other
Abies nordmanniana (Steven) Spach	✓	✓		
Cedrus libani A. Rich.	✓	✓		
Cephalotaxus fortunei Hook.	✓	✓		
Cunninghamia lanceolata (Lamb.) Hook.	✓			
Elymus repens (L.) Gould	✓		✓	
Equisetum telmateia Ehrh.			✓	Branches
Pinus sylvestris L.	✓	✓		
Poa trivialis L.	✓		✓	
Prumnopitys andina (Poepp. & Endl.) de Laub.	✓	✓		
Pteridium aquilinum (L.) Kuhn	✓		✓	
Quercus robur L.	✓	✓		
Rubus fruticosus L.	✓		✓	
Torreya californica Torr.	✓			
Wollemia nobilis W. G. Jones, K. D. Hill & J. M. Allen	✓	✓		

was photographed as a series of 16 overlapping images, using transmitted light, and the images saved in tagged image file format (TIFF).

Images were processed using ImageJ 1.47t (Rasband, 2013; Fig. 2). Each image consisted of a 1 × 1-cm square, and adjacent areas overlapping with other images from that sample. Most images contained some areas in which particle morphology was obscured, either by the density of the particles causing them to touch or overlap, or in some cases due to other material being present in the sample, or due to faults with the image itself. A region of interest, in which no distorted particle images were apparent, was therefore defined within each 1 × 1-cm square, and the remainder of the image deleted. The edited images were converted to 8-bit grayscale, and then binarized using the default IsoData algorithm (Ridler and Calvard, 1978), adjusting the maximum threshold value manually to distinguish the charcoal particles, and with the minimum threshold value set at 0. A series of shape descriptors were generated for all the resulting particle images. These included projected area, Feret diameter (defined as the longest straight line obtainable within the particle image), circularity, and aspect ratio.

Circularity was calculated according to the following formula, which results in values between 0 and 1, where 1 is a perfect circle and 0 an infinitely elongated polygon.

$$Circularity = 4\pi \times \frac{Area}{Perimeter^2}$$

Aspect ratio was calculated as the ratio of the major and minor axes of the best-fitting ellipse.

$$Aspect\ Ratio = \frac{major\ axis}{minor\ axis}$$

Particles of less than 315 μm² or greater than 1,000,000 μm² were excluded from the analysis. The lower limit serves to remove data derived from images of between one and nine pixels, from which meaningful information is unlikely to be obtained even for the most basic parameter of area (Francus and Pirard, 2004). It is also likely that images of this size would not have been easily visible during selection and thresholding, and they may not represent actual charcoal particles. The upper limit, which approximately coincides with the distinction between mesocharcoal and macrocharcoal as defined by Scott (2010), is essentially arbitrary. Particles at the high end of the size distribution were not present in sufficient numbers to produce statistically meaningful data, and their morphology may largely reflect the size and shape of the original sample cut, rather than the effects of internal structure and breakdown regime with which we are concerned.

All statistical tests were conducted using SPSS version 21.0 (IBM Corporation, 2012).

RESULTS

Variation in particle morphology was evident between the samples prior to measurement. Figure 3 is indicative of the variation in particle morphology visible to the naked eye, while representative images for each of the 26 specimens are given in Appendix S2. An average of 322 particles were measured from each sample, with a minimum of 30 and a maximum of 659.

All specimens exhibit a decrease in mean particle area with increasing time of simulated transport (see Appendix S1 for data and Appendix S3 for graphical representations). Mean particle area (Fig. 4) is plausibly modeled as a logarithmic function of transportation time ($r^2 > 0.8$) for the leaves of all species,

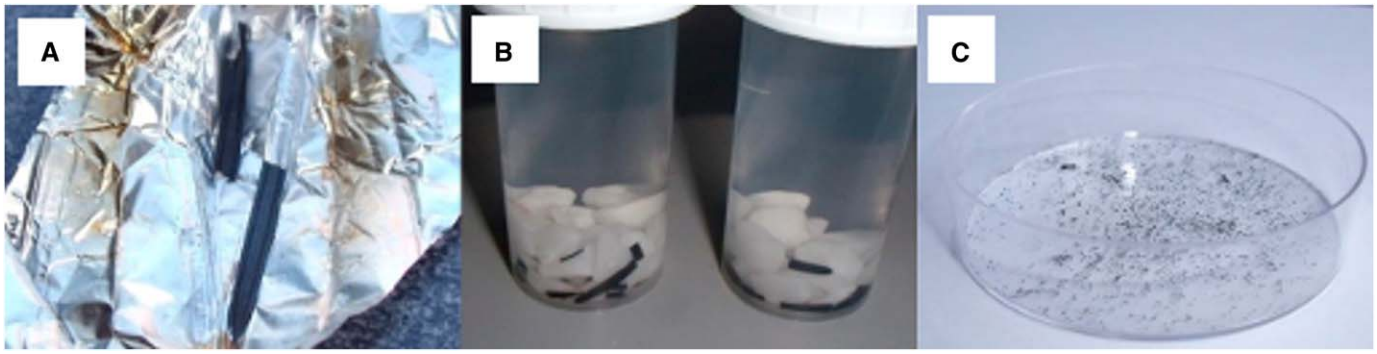

Fig. 1. Charcoal samples, as removed from furnace (A), prior to simulated transport with water and gravel (B), and dispersed on a Petri dish prior to imaging (C).

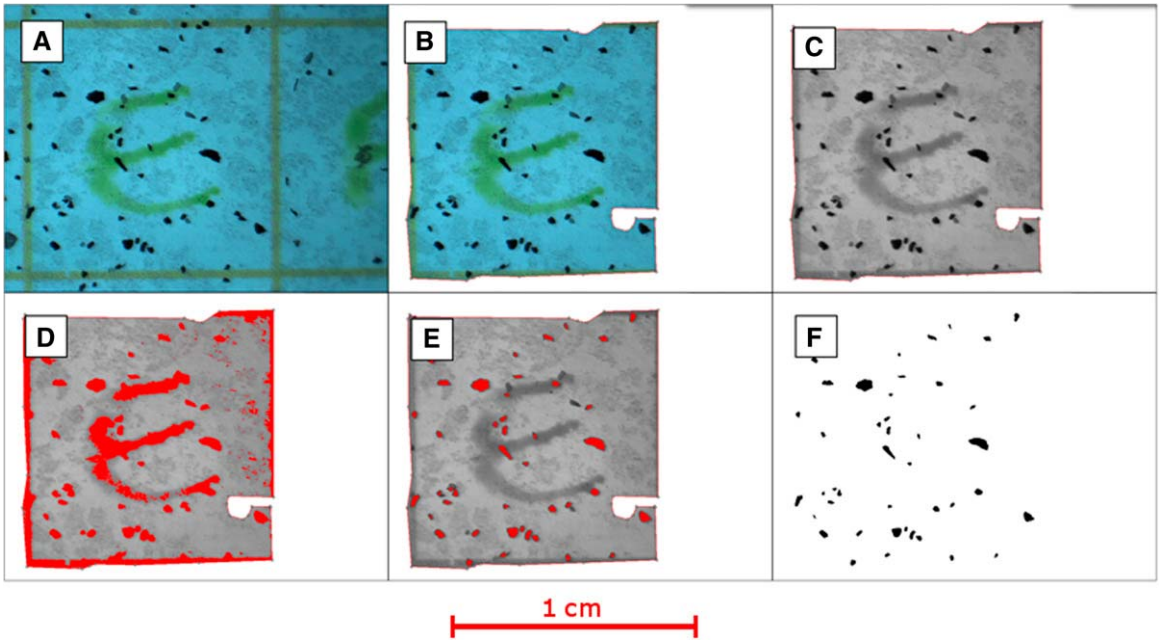

Fig. 2. Stages of image processing: a raw image overlapping with other images from the same sample (A); cropped to remove overlap with other images and overlapping particles (B); converted to 8-bit grayscale (C); with automatic thresholding applied (D); with threshold manually adjusted (E); and final binary image (F).

with the exception of *Poa trivialis* L., with a marked decrease in the rate of attrition generally evident between one and two hours. The branches of *Equisetum telmateia* Ehrh. also follow this trend. The mean particle areas of charcoal produced from stems or wood display generally low r^2 values when a logarithmic function is fitted; below 0.8 with the exceptions of *Cephalotaxus fortunei* Hook. and *Elymus repens* (L.) Gould. This apparent divergence of r^2 values between leaves (including

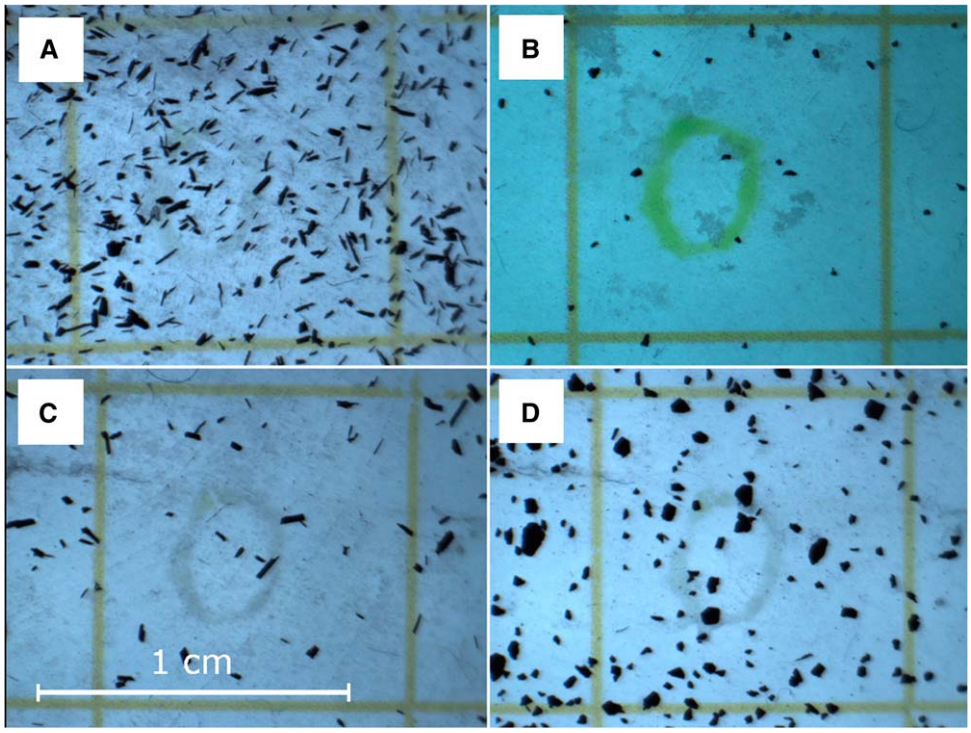

Fig. 3. Charcoal particles after four hours of simulated transport, showing variations in morphology visible to the naked eye: *Equisetum telmateia* stem (A), *Cedrus libani* wood (B), *Elymus repens* stem (C), and *Rubus fruticosus* leaf (D).

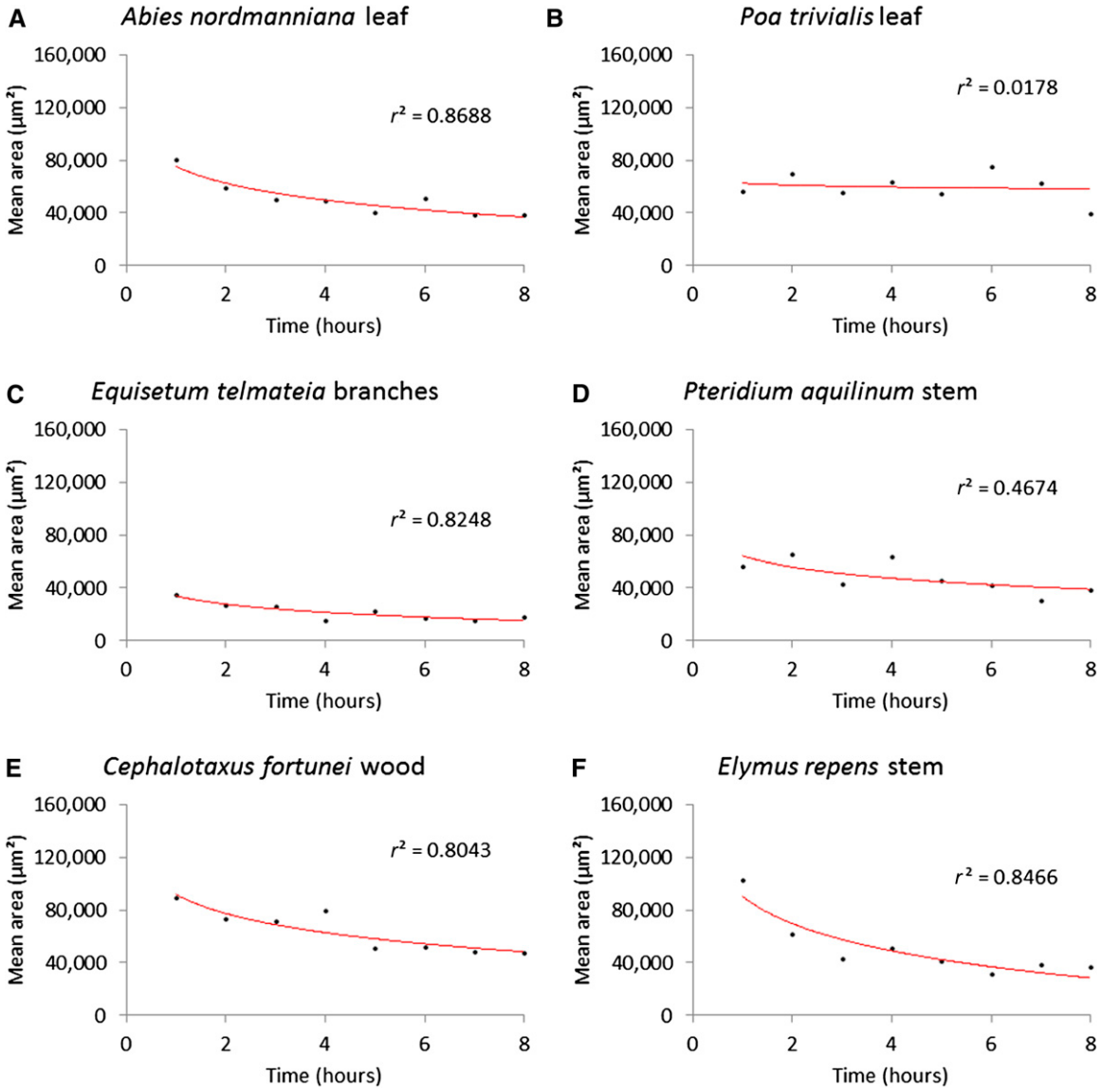

Fig. 4. Relationships between mean projected area and duration of simulated transport for charcoal particles (315–1,000,000 µm^2) produced from six of the plant materials. Logarithmic models and associated coefficients of determination (r^2) are also shown. *Abies nordmanniana* (A) is typical of the leaves (median r^2), showing mean particle area as a logarithmic function of transportation time; *Poa trivialis* (B) was the only leaf that did not display such a trend, although branches of *Equisetum telmateia* (C) did display this trend. *Pteridium aquilinum* (D) is typical of the stem samples (closest to median r^2) in fitting the logarithmic model poorly; *Cephalotaxus fortunei* (E) and *Elymus repens* (F) were exceptions to this.

Equisetum telmateia branches) and stems (including woody samples) was highly significant ($P < 0.001$; independent samples Mann–Whitney test). The Mann–Whitney test was employed due to a combination of nonnormal data distributions and small sample sizes.

All the leaf samples display an increase in mean circularity with increasing transport time (Fig. 5; Appendix S4). This tendency is less distinct than is the case for mean area; some r^2 values are low, and the *Equisetum* branches, which appear to follow the trend for leaves regarding area, tend to decrease in circularity, although without a convincing model fit. Wood and stem samples display no overall trends. Logarithmic models give r^2 values of <0.3 for all conifer woods, 0.7111 for *Quercus robur* L., 0.7323 for *Elymus repens*, and <0.4 for all other stem samples. Divergence in r^2 values between the two groups was significant ($P = 0.002$).

Aspect ratio generally decreases with time for leaf samples; the exceptions being *Cedrus libani* A. Rich. and *Quercus robur*, both of which display consistently low aspect ratios (Fig. 6; Appendix S5). Stem and wood samples display little consistency in relationships of aspect ratio to time. Few samples in either group display apparent trends in aspect ratio with transportation time, and when logarithmic models are fitted, divergence in r^2 between groups is not significant at a 95% confidence level ($P = 0.095$).

The samples were divided into four broad material types (grass, tree leaves, wood, and other) to assess differences in aspect ratio. Disregarding the degree of simulated transport undergone, the four types show distinctive differences in their distributions of aspect ratio (Fig. 7), with the grass charcoal having generally higher aspect ratios (mean 3.70) than the other fuel types (leaves 2.23, wood 1.97, other 2.70).

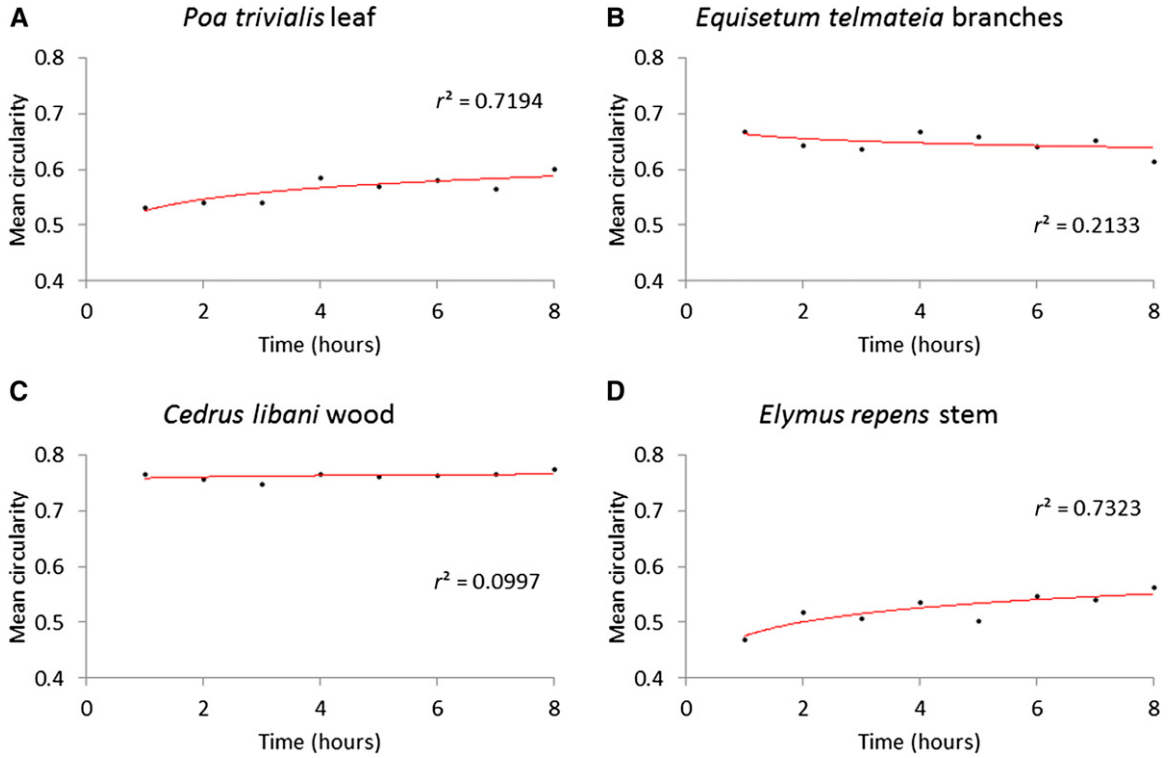

Fig. 5. Relationships between mean circularity and duration of simulated transport for charcoal particles (315–1,000,000 μm^2) produced from four of the plant materials. Logarithmic models and associated coefficients of determination (r^2) are also shown. *Poa trivialis* (A) is typical of the leaves (median r^2), showing an increase in mean circularity with increasing transport time. Although all true leaves displayed this tendency, charcoal particles from branches of *Equisetum telmateia* (B) did not. Stem samples showed no overall trends, with low coefficients of determination and inconsistent direction of change, with *Cedrus libani* (C) being typical (closest to median r^2). *Elymus repens* (D) was one of only two specimens that did have a reasonable model fit, showing increasing circularity with transport time.

We compared differences in aspect ratio between the four groups at each of 10 size fractions, according to Feret diameter, from 0–100 μm to 900–1000 μm. The differences in mean aspect ratio between the four groups remain similar across the range of particle sizes (Fig. 8), although they are noticeably more closely grouped at the ≤100 μm range. The significance of the difference in aspect ratios between the four groups was tested for each of the size ranges. The one-way Kruskal–Wallis test was employed for this, as it was not possible to demonstrate homogeneity of variance between the groups. The overall difference across the groups was highly significant ($P < 0.001$) at every size range (Table 2). Pairwise comparisons are also highly significant in most cases, with only seven out of 60 P values exceeding 0.001 (Table 2).

DISCUSSION

The natural transportation processes undergone by charcoal particles are potentially wide-ranging in terms of imposed energy as well as duration, and may include aeolian as well as hydrological transport. The degree to which our laboratory process replicates the forces that have acted upon any real charcoal assemblage may therefore be highly variable. The effects produced in this study will most likely correspond to those in charcoal particles that have undergone vigorous fluvial transport. During fluvial transport, charcoal will be subject to attrition as would any other material. Collisions with entrained sediment will cause abrasion of the surface and impart stresses in the charcoal that may lead to fracturing. The effect of these processes will be dependent on the concentration, hardness, and kinetic energy of the sediment. Hydraulic action and cavitation may also act upon the particles in a high-energy fluvial environment; but these are not expected to have had any effect in the laboratory simulation here, as tests without gravel in the samples resulted in no discernable breakdown of the charcoal. Floating or suspension of charcoal might be expected to minimize abrasion during hydrological transport. In our study, charcoal particles did not float after breakdown, with the exception of *Quercus robur* leaf charcoal, although the charcoal pieces typically did float before undergoing any simulated transport. In a natural situation, the kind of breakdown process simulated here might therefore be initiated after a period of relatively nondestructive transportation; however, having been initiated, the effect of the breakdown on buoyancy would serve to keep the particles submerged and, therefore, subject to further breakdown.

The majority of macroscopic (>1 mm) charcoal undergoes transportation by water (Scott, 2010), and it is also likely to be a common process for smaller particles. Fluvial transport may be enhanced by the influence of wildfires, which can alter hydrological behavior. Fire tends to decrease soil infiltration and increase overland flow, while at the catchment scale increasing runoff and reducing response time (Shakesby and Doerr, 2006), all of which will assist in carrying the charcoal produced into fluvial systems. Our fragmentation results may be applicable to charcoal assemblages that have undergone quite different

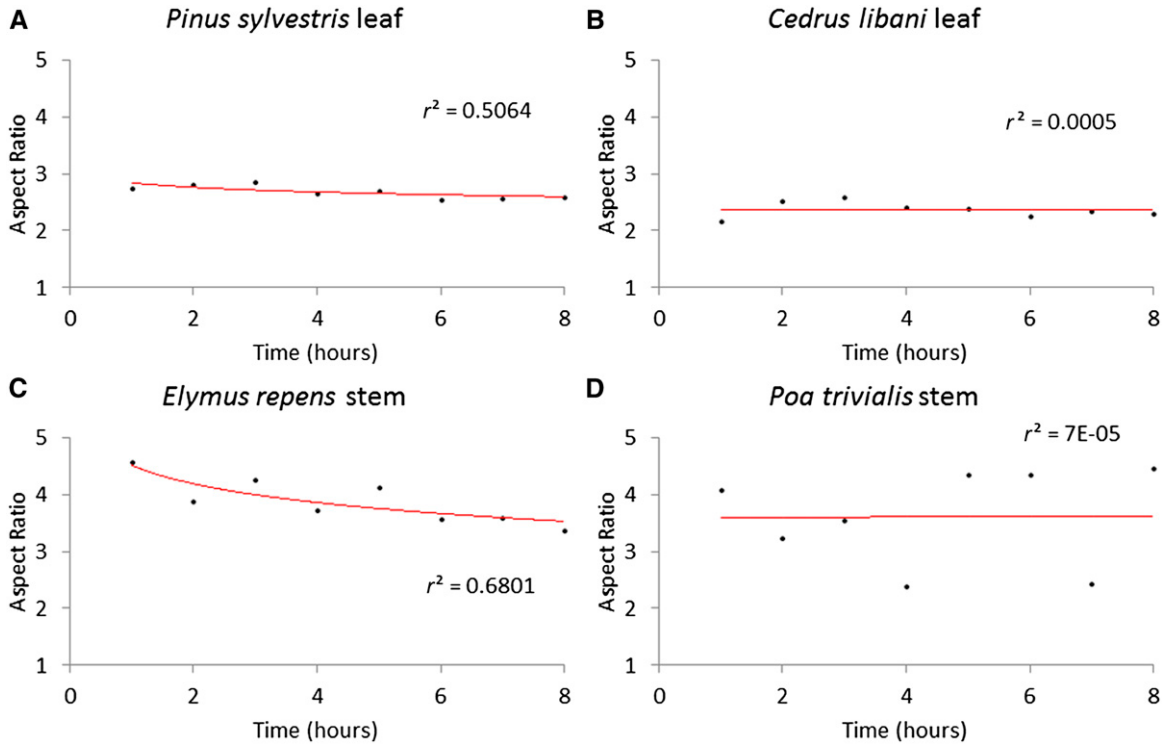

Fig. 6. Relationships between mean length : width ratio (calculated from the best-fitting ellipses) and duration of simulated transport for charcoal particles (315–1,000,000 μm^2) produced from four of the plant materials. Logarithmic models and associated coefficients of determination (r^2) are also shown. For leaf charcoal, aspect ratio generally decreased with increasing time, although r^2 values varied widely; *Pinus sylvestris* (A) is typical (median r^2). *Cedrus libani* (B) was one of two leaf specimens for which aspect ratio increased; neither show a convincing model fit. Stem samples showed no consistency in relationship of aspect ratio to time; the closest to a logarithmic relationship being *Elymus repens* (C) and the least well defined being *Poa trivialis* (D).

transportation processes, such as aeolian transport, mass movement of dry material, or a combination of processes, as the morphology of particles after breakdown may be determined primarily by internal structure. Regardless of the type of transportation that a natural charcoal assemblage has undergone, the effect in modifying particle morphology will vary according to the length of time spent in that environment. We do not attempt to relate length of simulated transport in this study to any measure of transportation time or distance of charcoal created by natural fires. However, the logarithmic changes in projected area and circularity, which are generally evident in the leaf charcoal samples, indicate that the period of substantive change has been captured in these cases.

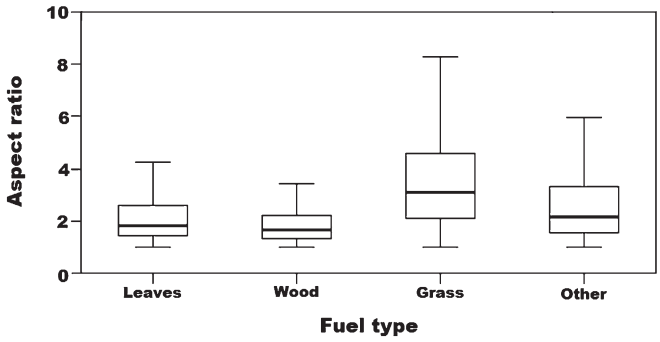

Fig. 7. Boxplot showing differences in distribution of aspect ratios (calculated from the best-fitting ellipses) of charcoal particles (315–1,000,000 μm^2), grouped into four broad material types. Outliers and extreme values are not shown.

In our experiments, the kinetic energy imparted to each sample remains constant through time. Therefore, the emergence of a logarithmic decrease in mean area, which is evident for the leaf samples, implies a decrease in the susceptibility of the particles to breakdown. In this respect, the results mirror those of Nichols et al. (2000), who attributed the decline in breakdown of their macrocharcoal samples to the removal of bark, leaving the less fragile wood charcoal beneath remaining much in its original shape. Because the logarithmic decrease was evident primarily in our leaf charcoal, a comparable distinction between two parts of the material cannot be drawn, although some other source of variability in the resistance of the leaf charcoal could be responsible. It is also possible that the size itself determines the susceptibility of the particles to breakdown under this regime, so that as they are reduced in size the rate of attrition declines regardless of the other physical properties of the charcoal.

It is to be expected that abrasion will cause circularity to increase as area decreases. Aspect ratio might be expected to decrease with decreasing area, because elongation of a particle may make fracturing more likely. The stresses that cause a particle to fracture are proportional to the force applied, and inversely proportional to the area resisting the force. Therefore, stresses are greatest, and fractures more likely, at cross-sections of lower area, at least in particles of homogeneous material; this

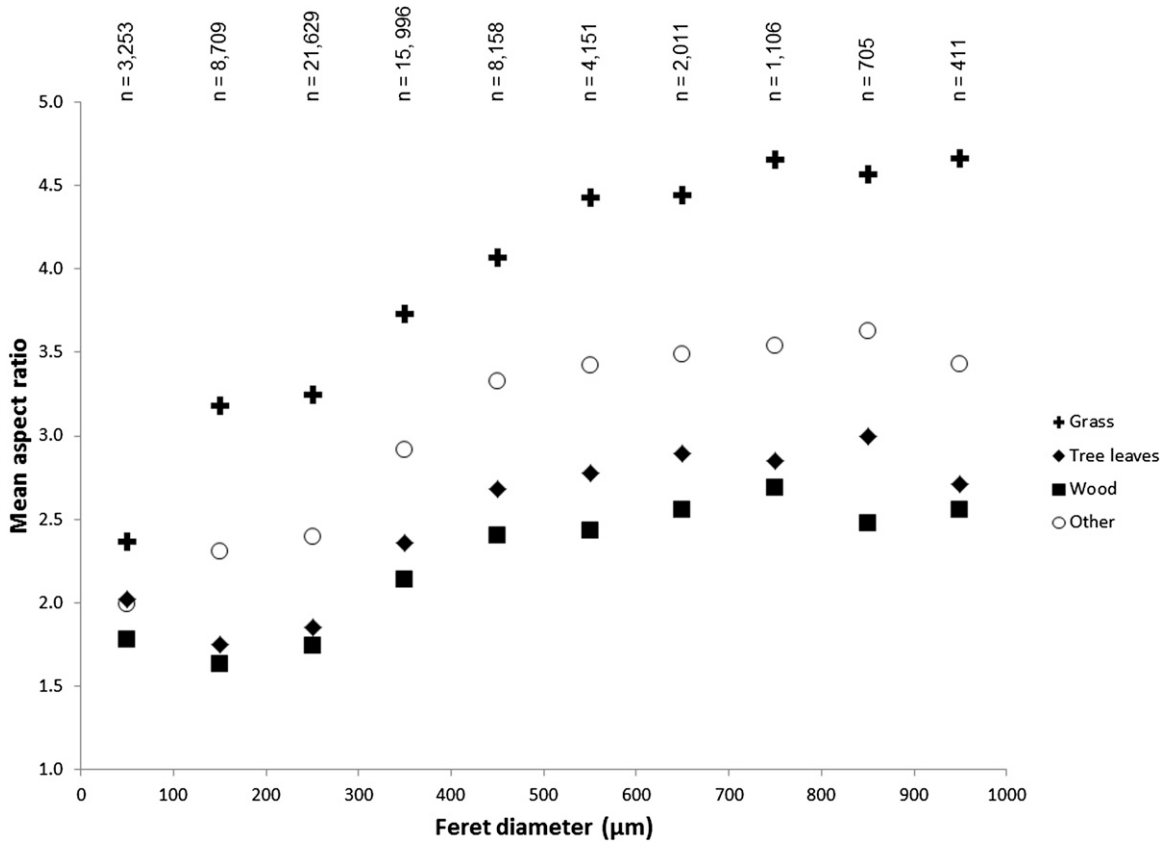

Fig. 8. Relationship of mean aspect ratio (calculated from the best-fitting ellipses) and Feret diameter of charcoal particles (315–1,000,000 µm^2), grouped into four broad material types. Feret diameters are grouped in ranges of 100 µm and plotted as the midpoint of each range.

should result in a decrease in elongation over successive breakages. However, this principle may well be overridden by the internal structure of the particles, especially if elongation of the particle reflects the presence, and follows the orientation, of more-resistant fibrous material within the sample. No simple relationship was identifiable between aspect ratio and time. The failure to find such a relationship may, however, be a consequence of imaging and measurement biases that affect this parameter in particular. Particles of very high aspect ratio may be lost during thresholding, where those of lower aspect ratio but similar size are retained.

The lack of an identifiable relationship between either area or circularity and transport time for wood or stem samples is consistent with the results of Nichols et al. (2000) in the simulated transport of *Pinus sylvestris* wood charcoal at a larger size fraction. This may be the result of a more heterogeneous nature of wood charcoal compared to leaf charcoal. It is notable, however, that the same results were obtained for rigid but non-woody stems (*Equisetum telmateia*, *Pteridium aquilinum* (L.) Kuhn, and *Rubus fruticosus* L.) as for the wood charcoal; while the *Equisetum* branches, which were the only nonrigid samples charcoalified other than leaves, followed the logarithmic trend for mean area. The *Equisetum* branches did not follow the logarithmic trend for circularity, but in this case some leaf samples did not either. This suggests that the factor determining whether a simple mathematical relationship exists between these morphological parameters and degree of breakdown is related more to the physical characteristics of the material than the function of the plant organ.

Umbanhowar and McGrath (1998) concluded that the mean aspect ratio of the best-fitting ellipse is a usable indicator of whether an assemblage of charcoal particles (125–250 µm) originated from a grassland fire or a forest fire. This conclusion was based on data from 16 species of grasses and deciduous trees native to Minnesota, USA, and is not necessarily applicable in other environments supporting different species. Our results show distinct variability in the distribution of aspect ratios between the four categories of grasses, tree leaves, wood, and other materials (Fig. 7). In keeping with the findings of Umbanhowar and McGrath (1998), it is the grass charcoal that displays the most distinctive distribution, with the highest aspect ratios.

Umbanhowar and McGrath (1998) specifically identified the mean aspect ratio of the 125–250-µm fraction as indicative of fuel type, based on the significance of the differences in distribution. Our particles were not physically sieved into different fractions, and so identifying this specific size fraction within our data is not possible. However, by dividing the particles into size fractions according to Feret diameter, it was possible to demonstrate that significant differences in aspect ratio between broad plant material types (grass, tree leaves, wood, other) are found across the range of diameters examined (Fig. 8).

With P values of <0.001 at each fraction, our results suggest that differences in aspect ratio between fuel types tend to be highly significant at a range of sizes. Pairwise comparisons reach the same level of significance in 53 out of 60 cases. Of the seven exceptions, only one comparison included grass charcoal; paired with other materials, this yielded a P value of 0.021

TABLE 2. *P* values obtained from Kruskal–Wallis tests on aspect ratios of four different fuel types, at each of 10 particle size ranges. All *P* values are unadjusted.

Feret diameter (μm)	Significance	Pairwise comparison	Pairwise significance
≤100.000	<0.001	Wood–leaves	<0.001
		Wood–other	<0.001
		Wood–grass	<0.001
		Leaves–other	0.877
		Leaves–grass	<0.001
		Other–grass	<0.001
100.001–200.000	<0.001	Wood–leaves	0.32
		Wood–other	<0.001
		Wood–grass	<0.001
		Leaves–other	<0.001
		Leaves–grass	<0.001
		Other–grass	<0.001
200.001–300.000	<0.001	All pairs	<0.001
300.001–400.000	<0.001	All pairs	<0.001
400.001–500.000	<0.001	All pairs	<0.001
500.001–600.000	<0.001	All pairs	<0.001
600.001–700.000	<0.001	All pairs	<0.001
700.001–800.000	<0.001	Wood–leaves	0.097
		Wood–other	<0.001
		Wood–grass	<0.001
		Leaves–other	<0.001
		Leaves–grass	<0.001
		Other–grass	<0.001
800.001–900.000	<0.001	Wood–leaves	<0.001
		Wood–other	<0.001
		Wood–grass	<0.001
		Leaves–other	0.021
		Leaves–grass	<0.001
		Other–grass	<0.001
900.001–1000.000	<0.001	Wood–leaves	0.188
		Wood–other	<0.001
		Wood–grass	<0.001
		Leaves–other	0.004
		Leaves–grass	<0.001
		Other–grass	0.021

at the 900–1000-μm range. While this is in any case sufficient to retain the hypothesis of distinct distributions at a 95% confidence level, it is noted that the higher *P* value is likely to be the result of the low number of particles present in this size range; the comparison in question involves a total particle number of 173. More generally, those comparisons where $P > 0.001$ are clustered at the lower and higher ends of the size distribution, where sample numbers were smaller.

While 125–250 μm is a typical fraction used for charcoal studies, both smaller and larger fractions are commonly used (e.g., Belcher et al., 2005; Olsson et al., 2010). Therefore, this demonstration that grass charcoal displays higher aspect ratios at a wider range of sizes will enable the application of this principle to a wider range of studies. In addition to showing that this method is not limited to a narrow size fraction, our results show it to be applicable to coniferous as well as broadleaved tree species. The fact that the difference in aspect ratios is demonstrated here using a very different method of charcoal breakdown than that of Umbanhowar and McGrath (1998) indicates that this method is likely not restricted to a narrow range of taphonomic processes.

While the mean aspect ratios for our grass charcoal samples range from 2.36 to 4.66, increasing with the size fraction, Umbanhowar and McGrath (1998) found a mean aspect ratio of 3.62 at 125–250 μm. It would be unreasonable to suppose that these two studies have captured the full range of aspect ratios that may be produced from different grass taxa under varying growth and burn conditions and taphonomic processes. It should also be noted that a natural charcoal assemblage is unlikely to consist of charcoal entirely from one type of vegetation, and so the elongation of particles in laboratory-produced grass charcoal may be unrealistically high. It is therefore not possible to specify a threshold ratio at which charcoal particles are indicative of grassland fire, and the practical application of the principle is likely to rely on corroboration from other sources of evidence.

This is demonstrated by the work of Daniau et al. (2013), who argue that periods that show an increase in microcharcoal aspect ratio in the Holocene record of southern Africa indicate an increase in grassland fire as a proportion of total biomass burning. By basing the analysis on relative changes in aspect ratio within a single sedimentary record, this approach avoids adopting a specific threshold ratio from another study, and by relating changes in fire regime to another relevant parameter (in this case Milankovitch cycles) obtains greater certainty through corroboration.

CONCLUSIONS

Our experiments indicate that charcoal formed from leaves displays more easily definable changes in morphological parameters than that formed from rigid or woody plant materials. Our data support the idea that the mean aspect ratio of a charcoal

assemblage can provide information about whether it originates from a grassland or woodland fire. The measurement of the aspect ratios of fossil charcoals using high-resolution image analysis provides a simple method for estimating their broad botanical affinities. A large amount of morphological data can be gleaned from fossil charcoal assemblages found in soils, sediments, and rocks, and when coupled to quantitation of charcoal abundance this approach may allow advances in our ability to make paleoecological and paleoenvironmental interpretations using the fossil record.

LITERATURE CITED

Belcher, C. M., M. E. Collinson, and A. C. Scott. 2005. Constraints on the thermal energy released from the Chicxulub impactor: New evidence from multi-method charcoal analysis. *Journal of the Geological Society* 162: 591–602.

Belcher, C. M., S. W. Punyasena, and M. Sivaguru. 2013. Novel application of confocal laser scanning microscopy and 3D volume rendering toward improving the resolution of the fossil record of charcoal. *PLoS ONE* 8: e72265.

Clark, J. S. 1988. Particle motion and the theory of charcoal analysis: Source area, transport, deposition, and sampling. *Quaternary Research* 30: 67–80.

Conedera, M., W. Tinner, C. Neff, M. Meurer, A. F. Dickens, and P. Krebs. 2009. Reconstructing past fire regimes: Methods, applications, and relevance to fire management and conservation. *Quaternary Science Reviews* 28: 555–576.

Daniau, A.-L., M. F. S. Goñi, P. Martinez, D. H. Urrego, V. Bout-Roumazeilles, S. Desprat, and J. R. Marlon. 2013. Orbital-scale climate forcing of grassland burning in southern Africa. *Proceedings of the National Academy of Sciences, USA* 110: 5069–5073.

Falcon-Lang, H. J. 1999. The Early Carboniferous (Courceyan–Arundian) monsoonal climate of the British Isles: Evidence from growth rings in fossil woods. *Geological Magazine* 136: 177–187.

Francus, P., and E. Pirard. 2004. Testing for sources of errors in quantitative image analysis. *In* P. Francus [ed.], Image analysis, sediments and paleoenvironments, 87–102. Springer, Dordrecht, The Netherlands.

Glasspool, I. J., D. Edwards, and L. Axe. 2004. Charcoal in the Silurian as evidence for the earliest wildfire. *Geology* 32: 381–383.

Higuera, P. E., M. E. Peters, L. B. Brubaker, and D. G. Gavin. 2007. Understanding the origin and analysis of sediment-charcoal records with a simulation model. *Quaternary Science Reviews* 26: 1790–1809.

Higuera, P. E., D. G. Gavin, P. J. Bartlein, and D. J. Hallett. 2010. Peak detection in sediment-charcoal records: Impacts of alternative data analysis methods on fire-history interpretations. *International Journal of Wildland Fire* 19: 996–1014.

IBM Corporation. 2012. IBM SPSS Statistics for Windows, Version 21.0. IBM Corporation, Armonk, New York, USA.

Jensen, K., E. A. Lynch, R. Calcote, and S. C. Hotchkiss. 2007. Interpretation of charcoal morphotypes in sediments from Ferry Lake, Wisconsin, USA: Do different plant fuel sources produce distinctive charcoal morphotypes? *The Holocene* 17: 907–915.

Marlon, J. R., P. J. Bartlein, M. K. Walsh, S. P. Harrison, K. J. Brown, M. E. Edwards, P. E. Higuera, et al. 2009. Wildfire responses to abrupt climate change in North America. *Proceedings of the National Academy of Sciences, USA* 106: 2519–2524.

McElwain, J. C. 1998. Do fossil plants signal palaeoatmospheric CO_2 concentration in the geological past? *Philosophical Transactions of the Royal Society of London. Series B, Biological Sciences* 353: 83–96.

Mooney, S. D., and W. Tinner. 2011. The analysis of charcoal in peat and organic sediments. *Mires and Peat* 7: 1–18.

Moore, P. D. 1989. No smoke without fire. *Nature* 342: 226–227.

Nichols, G. J., J. A. Cripps, M. E. Collinson, and A. C. Scott. 2000. Experiments in waterlogging and sedimentology of charcoal: Results and implications. *Palaeogeography, Palaeoclimatology, Palaeoecology* 164: 43–56.

Olsson, F., M.-J. Gaillard, G. Lemdahl, A. Greisman, P. Lanos, D. Marguerie, N. Marcoux, et al. 2010. A continuous record of fire covering the last 10,500 calendar years from southern Sweden: The role of climate and human activities. *Palaeogeography, Palaeoclimatology, Palaeoecology* 291: 128–141.

Orvis, K. H., C. S. Lane, and S. P. Horn. 2005. Laboratory production of vouchered reference charcoal from small wood samples and nonwoody plant tissues. *Palynology* 29: 1–11.

Peters, M. E., and P. E. Higuera. 2007. Quantifying the source area of macroscopic charcoal with a particle dispersal model. *Quaternary Research* 67: 304–310.

Rasband, W. S. 2013. ImageJ, Version 1.47t. U.S. National Institutes of Health, Bethesda, Maryland, USA.

Ridler, T. W., and S. Calvard. 1978. Picture thresholding using an iterative selection method. *IEEE Transactions on Systems, Man, and Cybernetics* 8: 630–632.

Scott, A. C. 2000. The Pre-Quaternary history of fire. *Palaeogeography, Palaeoclimatology, Palaeoecology* 164: 281–329.

Scott, A. C. 2010. Charcoal recognition, taphonomy and uses in palaeoenvironmental analysis. *Palaeogeography, Palaeoclimatology, Palaeoecology* 291: 11–39.

Scott, A. C., J. A. Cripps, M. E. Collinson, and G. J. Nichols. 2000. The taphonomy of charcoal following a recent heathland fire and some implications for the interpretation of fossil charcoal deposits. *Palaeogeography, Palaeoclimatology, Palaeoecology* 164: 1–31.

Scott, A. C., and F. Damblon. 2010. Charcoal: Taphonomy and significance in geology, botany and archaeology. *Palaeogeography, Palaeoclimatology, Palaeoecology* 291: 1–10.

Shakesby, R. A., and S. H. Doerr. 2006. Wildfire as a hydrological and geomorphological agent. *Earth-Science Reviews* 74: 269–307.

Umbanhowar, C. E. Jr., and M. J. McGrath. 1998. Experimental production and analysis of microscopic charcoal from wood, leaves and grasses. *The Holocene* 8: 341–346.

Whitlock, C., and S. H. Millspaugh. 1996. Testing the assumptions of fire-history studies: An examination of modern charcoal accumulation in Yellowstone National Park, USA. *The Holocene* 6: 7–15.